APPLICATION OF MULTIVARIATE CALIBRATION FOR SIMULTANEOUS DETERMINATION OF MAJOR AND MINOR CONSTITUENTS IN U_3Si_2 BY X-RAY FLUORESCENCE

Marcos A. Scapin, Clayton P. Silva, Marycel E. B. Cotrim and Maria Ap. F. Pires

Instituto de Pesquisas Energéticas e Nucleares (IPEN / CNEN - SP)
Av. Professor Lineu Prestes 2242
05508-000 São Paulo, SP
scapin@usp.br

ABSTRACT

The aim of this work is to establish and validate a methodology for a nondestructive quantitative chemical analysis method for simultaneous determination of the major constituents (U_{total} and Si) and impurities (B, Mg, Al, Cr, Mn, Fe, Co, Ni, Cu, Zn, Mo, Cd, etc.) present in U_3Si_2. The method must also meet the needs of nuclear reactors for the nuclear fuel qualification type, MTR, with low cost and analysis time, while also minimizing waste generation. For this purpose, an X-ray fluorescence technique will be applied. The technique is nondestructive, aside from sample preparation procedures that do not require previous chemical treatments (dissolving, digesting), and allows for fast chemical analysis. The fundamental parameters (FP) method was applied to corrections for spectral and matrix effects. The calibration model was obtained via principal component analysis using orthogonal decomposition by the singular value decomposition method (SVD) in U_3O_8 and U_3Si_2 samples. The results were compared by means of statistical tests in accordance with ISO 17025 on CRMs of U_3O_8 from New Brunswick Laboratory (NBL) and 16 U_3Si_2 samples provided by CCN of IPEN/CNEN-SP. Multivariate calibration is a promising method for determination of major and minor constituents in U_3Si_2 and U_3O_8 nuclear fuel, because the precision and accuracy are statistically equivalent to volumetric analysis (U_{total} determination), gravimetric analysis (Si determination), and ICP-OES methods (impurities determination).

1. INTRODUCTION

The first multi-purpose research nuclear reactor in Brazil (RMB) will become operational in 2018. As its name implies, the equipment, estimated at US $500 million, has multiple purposes. These purposes include production of radioisotopes for use in nuclear medicine for cancer exams/treatment and for research in the fields of nuclear technology, energy, agriculture, industry, materials science, and environment.

Furthermore, the RMB will have a large neutron flux intensity, enough to test fuel and materials used in reactors for power generation and propulsion, providing greater security to projects and ensuring continuity in the country's nuclear knowledge development [1].

In Brazil, about 2 million radiopharmaceutical procedures are performed each year. About 80% of them use the radioisotope, technetium-99 (^{99}Tc), which is derived from molybdenum-99 (^{99}Mo). This raw material is imported because there is no national production. There are

other radioactive elements also used in health services whose demand is not fully met by the small research reactors operating in Brazil. In total, the cost for medical radioisotopes is greater than R $30 million annually. A reactor has an expected lifetime of 50 years; therefore, radioisotope production alone would be sufficient to repay the initial investment in 20 years [1].

The RMB would make Brazil self-sufficient in the sector, double the amount of radiopharmaceuticals offered to society, and allow for export of any surpluses. Brazil could then enter a restricted market, which is dominated today by institutions in Canada, South Africa, Holland, Belgium, and France, where more than 95% of [99]Mo is produced [1].

Beyond production of radiopharmaceuticals for medical purposes, the RMB will have a sufficient neutron flux to test fuels and materials used in power reactors and propulsion. This will provide greater security for these projects and ensure continuity in the development of the country's nuclear knowledge [1].

The technology to manufacture fuel for the RMB is already in place. The fuel will be plate type (Material Test Reactor (MTR)), with a U_3Si_2 base, and produced at the Nuclear and Energy Research Institute (IPEN-CNEN/SP) [2].

Currently, the production of MTR fuel begins by mixing aluminum with uranium silicide powder enriched to 20 wt% [235]U, in proportions predetermined. After, the mixture is compressed as briquettes and degassed under vacuum. Finally, one set of U_3Si_2-Al briquettes is mounted on laminate to constitute the fuel core, which is then encased in a frame with two revetments of aluminum (top and nether). To ensure quality, stringent tests are applied at all process stages [3, 4].

Although not an innovative technology, U_3Si_2, with 4.8 g U/cm^3, is currently the world's most advanced commercial fuel [2]. Its performance in reactors depends on the chemical composition and absence of impurities. Lack of impurities is a requisite for good neutron economy, because their presence compromises the fuel energy density [5, 6].

Elements with a high neutron capture cross section, such as B and Cd, absorb thermal neutrons. The alkali, alkaline earth, and transition metals can form oxides, modifying the metal to oxygen ratio in a fuel matrix [6, 7]. Moreover, when combined with even ultra-trace levels of rare earth elements, such as Sm, Eu, Gd, and Dy, a decrease in energy density is caused, since radionuclides can be produced after reactor irradiation [7, 8, 9].

There are many techniques to determine impurities in uranium compounds. Spectroscopic methods are used most often because they allow for simultaneous determination using a small sample amount. These methods present advantages and disadvantages based on spectral interferences, accuracy, cost, type of sample (solid or liquid), and equipment used for analysis. The method must take into consideration the detection limit, sample preparation, and steps required for pre-concentration [6, 10].

Two spectrophotometric methods used for impurity determination in uranium compounds are flame atomic absorption spectrometry (FAAS) and inductively coupled plasma optical emission spectrometry (ICP-OES), which are requires for the separation of uranium because

of spectral interferences. The uranium separation can be achieved using solvent extraction, precipitation, ion exchange chromatography, distillation, or electrolysis [11, 12, 13].

A review of the literature shows that ion chromatography can act as an alternative method to complement the currently applied separation techniques because of its versatility, ease of use, fast separation, selectivity, and sensitivity. It is a multi-element technique and has been widely used to analyze nuclear fuels, in both the final product and process materials. Transition metal ions can be analyzed by reverse-phase chromatography, cation/anion ion chromatography, and ion chromatography with chelation [6]. Transition metal cationic species separation must be done by complexation of the metal ions in the mobile phase to reduce the charge density effect. Commonly, weak organic acids such as citric acid, oxalic acid, and PDCA are used to reduce the positive charge of metal cations and increase the separation speed and efficiency [6, 7, 14].

No single analytical technique is ideal for determination of all the elemental impurities since most of the elements are present in ultra-traces levels, and sometimes techniques do not possess the detection limit required for determination of the analytes. Low concentrations of the impurities, in the range of $mg\ g^{-1}$ to $\mu g\ g^{-1}$, associated with uranium complex matrices as UO_2, U_3Si_2, U_3O_8, and U-MO, need to be determined, and compatible analytical methodologies must to be validated [6, 7, 14].

Thus, there is a need to develop rapid and simple methods for chemical characterization of materials used as nuclear fuel. In this context, the aim of this work is to evaluate the potential of wavelength dispersion X-ray fluorescence technique (WDXRF) for chemical characterization of nuclear materials in accordance with technical specifications for nuclear fuels made of U_3O_8 and U_3Si_2. The overall goal is to establish and validate a method for a non-destructive, inexpensive, and rapid quantitative chemical analysis, in addition to minimizing the generation of waste from simultaneous determination of the major constituents (U_{total} and Si) and impurities (B, Mg, Al, Cr, Mn, Fe, Co, Ni, Cu, Zn, Mo, Cd, and others) present in U_3O_8 and U_3Si_2 in accordance with ISO 17025.

2. EXPERIMENTAL

2.1. Sample preparation

The pressed powdered samples were prepared according to the following steps: 1.8 g of sample and 0.2 g of wax (wax C micro powder, Hoechst) were transferred to a polyethylene bottle (5 cm^3) and homogenized in a mechanical mixer for 5 min (Spex Mixer/Mill). The mixture was compacted by a hydraulic press (Herzog) using a pressure of 20 MPa for 2 s on a base of boric acid (H_3BO_3 PA) previously compressed with 100 MPa for 10 s. This gave pressed samples 25.01 ± 0.01 mm in diameter and 5.0 ± 0.2 mm in thickness.

2.2. Instrumental parameters

The experiments were carried out using a WDXRF spectrometer (RIGAKU Co., model RIX 3000) with the following primary devices: one 3 kW (Rh target) X-ray tube, 6 sample

positions, 4 kinds of primary X-ray filters for Al, Ti, Ni, and Zr, 3 divergence slits (160, 460, 560 μm), 8 diffracting crystals, and 2 detectors (scintillation and flow-proportional counters). The parameters such as excitation, emission line (EL), divergence slit (Ds), diffracting crystal (Dc), detector (D), fixed counting time (t), and Bragg's positions (2θ) for B, Mg, Al, Si, Ca, V, Cr, Mn, Fe, Co, Ni, Cu, Zn, Mo, Cd, Sn, Ba, Pb, and U are shown in Table 1.

Table 1: Measurement conditions for WDXRF

Excitation: 50kV x 50mA						2θ (graus)		
E	EL	Ds (μm)	Dc	D	t(s)	BG1	peak	BG3
B	B-K_α	560	RX70	FPC	200	44.000	49.280	56.000
Mg	Mg-K_α	560	TAP	FPC	200	44.850	45.190	45.650
Al	Al-K_α	560	PET	FPC	40	144.440	145.220	145.240
Si	Si-K_α	560	PET	FPC	40	108.30	109.235	109.630
Ca	Ca-K_α	560	Ge	FPC	40	60.860	61.260	61.660
V	V-K_α	560	LiF(200)	SC	40	76.710	76.910	77.110
Cr	Cr-K_α	560	LiF(200)	SC	20	69.130	69.330	69.530
Mn	Mn-K_α	560	LiF(200)	SC	20	62.750	62.950	63.150
Fe	Fe-K_α	160	LiF(200)	SC	20	57.300	57.505	57.700
Co	Co-K_α	560	LiF(200)	SC	20	52.570	52.770	52.970
Ni	Ni-K_α	160	LiF(200)	SC	20	48.450	48.650	48.850
Cu	Cu-K_α	560	LiF(200)	SC	20	44.810	45.010	45.210
Zn	Zn-K_α	160	LiF(200)	SC	20	41.580	41.780	41.980
Mo	Mo-K_α	560	LiF(200)	SC	20	20.120	20.320	20.250
Cd (F-Zr)	Cd-K_α	560	LiF(200)	SC	20	15.110	15.300	15.500
Sn	Sn-K_α	160	LiF(200)	SC	20	13.830	14.030	14.230
Ba	Ba-L_α	560	LiF(200)	SC	20	86.930	87.130	87.330
Pb	Pb-L_α	560	LiF(200)	SC	20	33.710	33.915	34.111
U	U-L_α1-2nd	560	LiF(200)	SC	20	53.560	53.765	53.960

TAP: Thallium Acid Phtalate, PET: Pentaerythritol, LiF: Lithium Fluoride, Ge: Germanium,
SC: Scintillation Detector, NaI/Tl - FPC: Flow-Proportional Counter, F-Zr: Zr primary X-ray filter.

2.3. Reference materials

The two sets of reference materials characterized for uranium matrix impurities were from the New Brunswick Laboratory (NBL) and labeled CRM 123(1–7), an 18 element impurity standard, and CRM 124(1–7), a uranium oxide standard with 24 trace elements [15].

One set of the sixteen U_3Si_2 reference samples (20% enriched in [235]U) were from 1999 to 2012 and provided by Nuclear Fuel Center (CCN) of IPEN/CNEN-SP. The samples were (SE 002/99 (A1), SE 003/07 (A2), SE 005/04 (A3) SE 006/04 (A4), SE 007/04 (A5), SE 010/08 (A6), SE 016/09 (A7), SE0 13/09 (A8), SE 014/09 (A9), SE 018/09 (A10), SE 011/09 (A11),

SE 019B/10 (A12), SE 020/10 (A13), SE 024/11 (A14), SE 023/11 (A15), and SE 028/12 (A16)), and their respective results were obtained by gravimetric analysis (for Si), volumetric analysis (for U_{total}), and ICP-OES (for B, Mg, Al, Si, Ca, V, Cr, Mn, Fe, Co, Ni, Cu, Zn, Mo, Cd, Ba, Sn, and Pb impurities).

2.4. Univariate calibration

First, a qualitative analysis was performed on CRM-124 (1) to check for interferences and set up instrumental conditions. The overlaps were corrected using filters and a deconvolution method. The overlap correction coefficients were calculated by Eq. 1.

$$Iic = Ii \sum LijIij$$

(1)

I_{ic} ≡ Intensity after overlap correction
I_i ≡ Intensity before overlap correction
L_{ij} ≡ Overlap correction coefficient for element j
I_{ij} ≡ Intensity of element j

The matrix correction coefficients (absorption/excitation) were calculated by the FP method, Eq. 2.

$$Wi = (aIi * Ii + bIi + C)\left\{ 1 + K + \sum AijFj + \sum QijkFjFk + \sum \frac{RijFj}{1 + W1} + \sum BijFj + \sum DijkFjFk + C \right\}$$

(2)

W_i ≡ Quantification value
a, b, c ≡ Calibration curve coefficients
I_i ≡ X-ray intensity
K ≡ Constant term
A_{ij} ≡ Absorption/excitation correction coefficient
F_j ≡ Analysis value or X-ray intensity of correction component
Q_{ij} ≡ Absorption/excitation correction coefficient (secondary correction)
R_{ij} ≡ Excitation correction coefficient
B_{ij} ≡ Overlap correction coefficient
D_{ij} ≡ Absorption/excitation correction coefficient
C ≡ Constant term

After setting up the instrumental conditions, seven measurements for B, Mg, Al, Si, Ca, V, Cr, Mn, Fe, Ni, Cu, Zn, Mo, Cd, Sn, and Pb were performed on CRM-123 (1–7). The net intensities of each element were related to their respective concentrations, and using linear regression the coefficients of each curve were calculated.
The methodology was evaluated using CRM-124 (1). Three samples were prepared, and six measurements for each element were performed. The following statistical tests were then applied.
At first, Chauvenet's test was applied for detection of outliers, according to Eq. 3 [16].

$$|X_i - \bar{X}| > k_n * s \tag{3}$$

X_i $\equiv$ Individual measured value
$\bar{X}$ $\equiv$ Average
k_n $\equiv$ Chauvenet's coefficient
s $\equiv$ Standard deviation

The precision was calculated in terms of relative standard deviation (RSD) and accuracy in terms of relative error (RE) and Z-score (Z), Eq. 4 [17].

$$Z = \frac{(\bar{X}_{Lab} - \bar{X}_{CRM})}{\sqrt{U^2_{Lab} - U^2_{CRM}}} \tag{4}$$

Z $\equiv$ Standard error
$\bar{X}_{Lab}$ $\equiv$ Experimental average
$\bar{X}_{CRM}$ $\equiv$ Certificate value
U^2_{Lab} $\equiv$ Experimental variance
U^2_{CRM} $\equiv$ Certificate variance

The limit of quantification (LoQ) was calculated according to Eq. 5 [18].

$$LoQ = 2 * \sqrt{\sum_{m=1}^{n} \frac{(C_m - \bar{C})^2}{n-1}} \tag{5}$$

2.5. Multivariate calibration

Under predetermined instrumental conditions, MCR-123 (1–7) samples were measured in 2θ scan mode. The spectra and concentration of each element were organized in a matrix, X and Y, respectively. The following parameters were calculated using MATLAB 7.0.1 [19].

Xm $\equiv$ mean vector (X variables)
Xcm $\equiv$ original matrix of autoscaled data
Xstd $\equiv$ standard deviations vector of X variables
Xa $\equiv$ original matrix of autoscaled data
V $\equiv$ loadings matrix
T $\equiv$ scores matrix
S $\equiv$ singular values
B $\equiv$ vector regression

The vector regression (b) provided the multivariate calibration curve for U_3O_8 samples. The methodology was evaluated using CRM-124 (1); three samples were prepared and six measurements were performed for each cited element. The same statistical tests described in 2.4 were applied.

The same process was applied to the U_3Si_2 samples, and a multivariate calibration curve was obtained. The quantification limit was calculated according to Eq. 5. The results obtained were compared with results from gravimetric (for Si), volumetric (for U_{total}), and ICP-OES

(for impurities) methods, using analysis of variance (ANOVA) to determine precision and the student t-test (paired t-test), at a 0.5 significance level, (Eq. 6) to determine accuracy.

$$t_{experimental} = \frac{(d - d_0)}{sd/\sqrt{n}}$$ (6)

d ≡ sample mean
d_0 ≡ mean value of differences in population tested
sd ≡ standard deviation
n ≡ sample size

2.6. Uncertainty evaluation

The sources of error associated with analytical procedures that can influence the analytical results are represented in a cause and effect diagram (Fig. 1). The central vector (C) represents the measurement and the ramifications and contributions from different factors that can affect the analysis results.
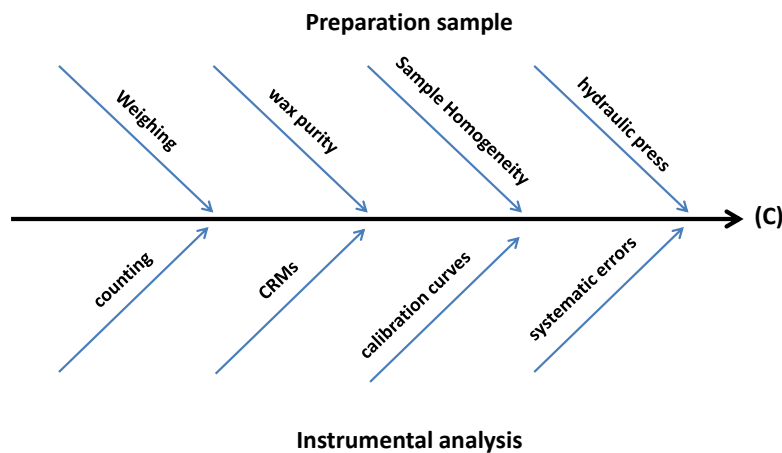
Figure 1: Cause and effect diagram showing sources of uncertainty associated with methods

The diagram shows that uncertainty sources related to sample preparation and instrumental parameters are independent. Thus, the uncertainty of the method was calculated in terms of combined uncertainty (u_c) according to Eq. 7 [20].

$$u_c = \sqrt{u_1^2 + u_2^2 + u_3^2 + \cdots . u_n^2}$$ (7)

u_c ≡ combined uncertainty
u_1^2 ≡ uncertainty of source 1
u_2^2 ≡ uncertainty of source 2
u_3^2 ≡ uncertainty of source 3

The combined uncertainty value (u_c) was multiplied by a coverage factor ($k = 2$). Application of a coverage factor of 2 corresponds to a confidence level of approximately 95% [20]. Thus, the expanded uncertainty has been calculated.

3. RESULTS AND DISCUSSION

The qualitative analysis results for CRM-124 (1) (Fig. 2) showed overlaps of U-Lβ1-2nd with Zn-Kα, ULβ1 with Mo-Kα, and Rh-Kβ1 with Cd-Kα; furthermore, the counting rate was low for lines corresponding to B-Kα, Mg-Kα, Al-Kα, Si-Kα, V-Kα, Cr-Kα, Mn-Kα, Cu-Kα, Zn-Kα, Cd-Kβ1, and S-Kα.

Figure 2: WDXRF Spectrum for CRM 124 (1)

A deconvolution method was applied to correct for overlap, with the exception of Cd-Kα where a Zr-filter was used. Subsequently, the FP method was applied for correction of the absorption/excitation effects.

3.1. Univariate calibration results

In Table 2, certified (Xcert ± σ) and determined values (Xdet ± σ; average and uncertainty), RSD, RE, LoQ, and Z-score (Z) for MRC 124 (1) − NBL are presented, along with the correlation coefficients (r^2) of the univariate calibration curves.

The correlation coefficients (r^2) for B (0.01), V (0.06), and Cd (0.17) are less than 1.00, indicating a correlation between intensity (counting rate) and concentration. The most likely hypothesis for any discrepancy is that the FP method used for absorption/excitation corrections was not effective, and that the Zr-filter used to correct the overlay of Rh-KB1 on Cd-Kα was also ineffective. Al (0.81), Mn (0.75), and Pb (0.81) are closer to 1.00, but still not satisfactory for the statistical tests applied. Thus, this methodology does not allow for quantification of B, Al, V, Mn, Cd, and Pb in the U_3O_8 matrix.

The elements with correlations >0.91 (Mg, Si, Ca, Cr, Fe, Ni, Cu, Zn, Mo, and Sn) had precisions values (RSD) between 5% and 13%, except for Mg (21%).

The accuracy in terms of RE is <10% for Mg, Ca, Cr, Ni, Zn, Sn, and Mo, whereas Si, Fe, and Cu had larger errors (56, 55, and 29%). However, there are no statistically significant differences between the determined and certified values since Z < 2 for all elements, except Fe (4.8).

Table 2: Certified (Xcert ± σ) and determined values (Xdet ± σ), RSD, RE, LoQ, Z-score (Z), and correlation coefficients (r^2) for CRM 124 (1)

| Elements	Xcert ± σ ($\mu g\ g^{-1}$)	Xdet ± σ ($\mu g\ g^{-1}$)	RSD (%)	RE (%)	LoQ ($\mu g.g^{-1}$)	Z	r^2
B	5.1±1.0	ND	NC	NC	NC	NC	0.01
Mg	101±13	105±22	21	4	36	0.3	0.98
Al	205±37	ND	NC	NC	NC	NC	0.81
Si	202±58	89±4	5	56	9	1.9	0.96
Ca	200±36	194±11	6	3	13	0.2	1.00
V	50.0±7.2	ND	NC	NC	NC	NC	0.06
Cr	102±14	108±8	7	6	13	0.4	0.98
Mn	51.0±7.6	ND	NC	NC	NC	NC	0.75
Fe	210±24	95±10	11	55	21	4.8	0.91
Ni	202±17	191±1	1	5	2	0.6	1.00
Cu	50.0±9.4	64±7	11	29	34	1.5	0.99
Zn	202±57	198±25	13	2	29	0.1	1.00
Mo	100.0±5.5	92±5	5	8	8	1.5	0.99
Cd	5.20±0.88	ND	NC	NC	NC	NC	0.17
Sn	51.0±6.9	55±3	6	7	6	0.5	1.00
Pb	51±15	ND	NC	NC	NC	NC	0.81

ND= Not Determined; NC= Not Calculated

This methodology is sensitive to impurities determination, with respect to the LoQ, since Si, Ni, Mo, and Sn are quantified at <10 $\mu g\ g^{-1}$; Ca, Cr, and Fe at <20 $\mu g\ g^{-1}$; and Mg, Cu, and Zn at <30 $\mu g\ g^{-1}$.

Thus, univariate calibration allows quantification of Mg, Si, Ca, Cr, Ni, Cu, Zn, Mo, and Sn impurities in U_3O_8 matrices.

3.2. Multivariate calibration with U_3O_8 CRM

The calibration model was constructed using the same set of MRC-123 (1–7) with the instrumental conditions presented in Table 1 using the 2θ scan method. The X matrix (intensity matrix) was obtained by averaging seven replicates for each element from all CRM measurements according to their respective energy (Fig. 3), resulting in a 7 × 19 matrix.
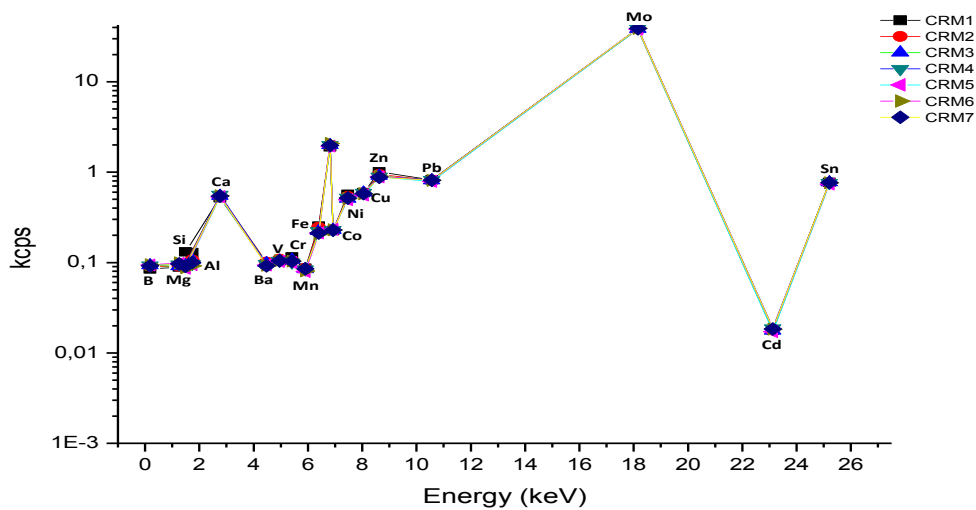
Figure 3: Intensity vs. Energy plot used to obtain an X matrix with U_3O_8 CRM

Using Matlab software (MatLab 7.0.1), the mean values and deviations pertaining to the centering matrix were calculated. Subsequently, a principal component analysis was performed to determine the number of components needed to describe data set. The results showed a main component is sufficient (PC1 = 99.9999%, PC2 = 0.0001%) [21]. In Fig. 4, loading versus energy, calculated for PC1, is shown.
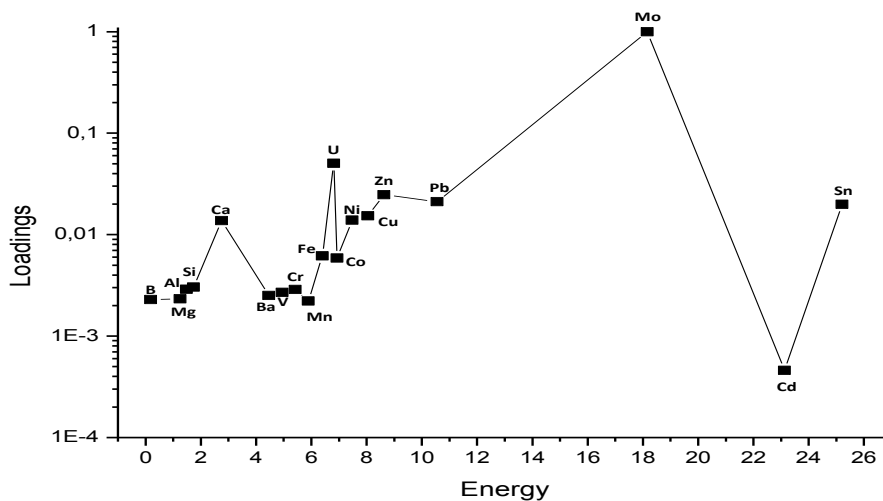
Figure 4: Loading vs. Energy for PC1 in U_3O_8

Comparison of Fig. 3 and Fig. 4 indicates that one component is sufficient to describe the whole set.

The calibration model was obtained using the partial least square (PLS) method [21], and statistical test validation was applied to CRM 124 (1).
In Table 3, certified (Xcert ± σ) and determined values (Xdet ± σ; average and uncertainty), RSD, RE, LoQ, and Z-score (Z) are presented for CRM 124 (1).

The precision assessment, in relation to the RSD, showed satisfactory repeatability for all elements determined (RSD ≤10%). According to the INMETRO recommendation, RSD values above 10% are considered unsatisfactory. The process was reproducible [17].

The accuracy evaluation, in relation to the Z-score (Z), presented values less than ≤1.9, making it satisfactory [17].

The limits of quantification (LoQ) also showed adequate values once they were lower than 3 $\mu g\ g^{-1}$ for B and Cd. These elements are of great interest because of their high cross sections. Furthermore, for all other elements the LQ is less than 90 $\mu g\ g^{-1}$, with the exception of Si (99 $\mu\ g^{-1}$).

**Table 3: Certified (Xcert ± σ) and determined values (Xdet ± σ), RSD, RE, LoQ, and Z-score (Z) for MRC 124 (1)**

| Elements	Xcert ± σ ($\mu g.g^{-1}$)	Xdet ± σ ($\mu g.g^{-1}$)	RSD (%)	RE (%)	LoQ ($\mu g.g^{-1}$)	Z
B	5.1±1.0	4.8±0.4	8	6	2.6	0.3
Mg	101±13	82±7	9	19	43	1.5
Al	205±37	166±14	8	19	81	1.1
Si	202±58	197±16	8	3	99	0.1
Ca	200±36	176±14	8	12	87	0.7
V	50.0±7.2	40±4	10	20	22	1.4
Cr	102±14	85±7	8	17	43	1.2
Mn	51.0±7.6	42±4	10	18	21	1.2
Fe	210±24	173±13	8	18	80	1.5
Ni	202±17	169±12	7	16	77	1.9
Cu	50.0±9.4	42±4	10	16	22	0.8
Zn	202±57	179±15	8	11	88	0.4
Mo	100.0±5.5	85±1	1	15	40	1.9
Cd	5.20±0.88	4.2±0.4	10	10	2	1.1
Sn	51.0±6.9	38±3	8	25	20	1.8
Pb	51±15	35±3	9	21	18	1.1

3.3. Univariate and multivariate calibration comparison

The comparison between univariate and multivariate calibrations was made based on precision (RSD), accuracy (Z-score), and LoQ calculated for CRM 124 (1).

The RSD (Fig. 5) for both methods is less than 10%, except for Mg (21%). Thus, it can be stated that the precision of the two methods is comparable. However, multivariate calibration has a higher precision for B, Mg, Al, V, Mn, Cd, and Pb determination.
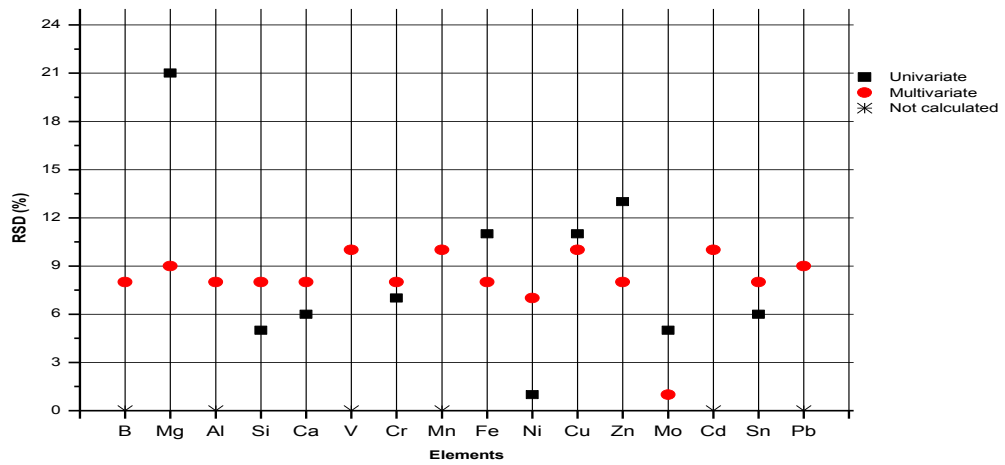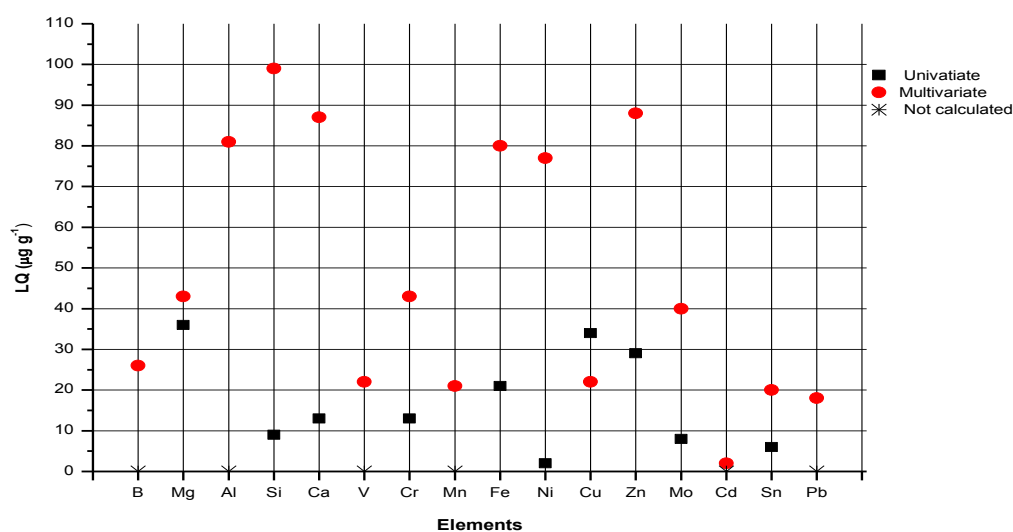
Figure 5: RSD comparison of univariate and multivariate calibrations
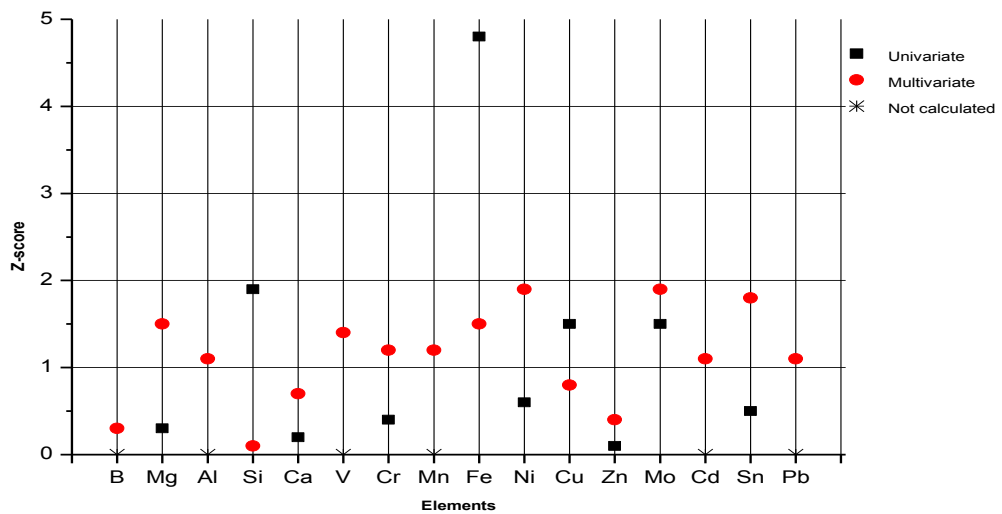
Figure 6: Comparison of the Z-score values for univariate and multivariate calibration

The Z-score values (Fig. 6) for both methods are <2, except for Cu (2.1) and Fe (4.8) using the univariate calibration. The results show that the accuracy of both methods is comparable; however, for Cu and Fe determination, multivariate calibration provides more reliable results (exact). Furthermore, for B, Al, V, Mn, Cd, and Pb, multivariate calibration has a greater accuracy.

The LoQ (Fig. 7) is lower for univariate calibration, except for Cu. However, multivariate calibration also has LOQ values sufficient for impurity determination in U_3O_8 matrices.

Figure 7: LoQ comparison for univariate and multivariate calibration

3.4. Multivariate calibration using U_3Si_2 reference samples

The calibration model based on the U_3Si_2 samples was built in the same manner as the model for U_3O_8, i.e. the instrumental conditions presented in Table 2 using the 2θ scan method. The X matrix (intensity matrix) was also obtained by averaging seven replicas from each sample for each element, according to its respective energy (Fig. 8), resulting in a 16 x 19 matrix.
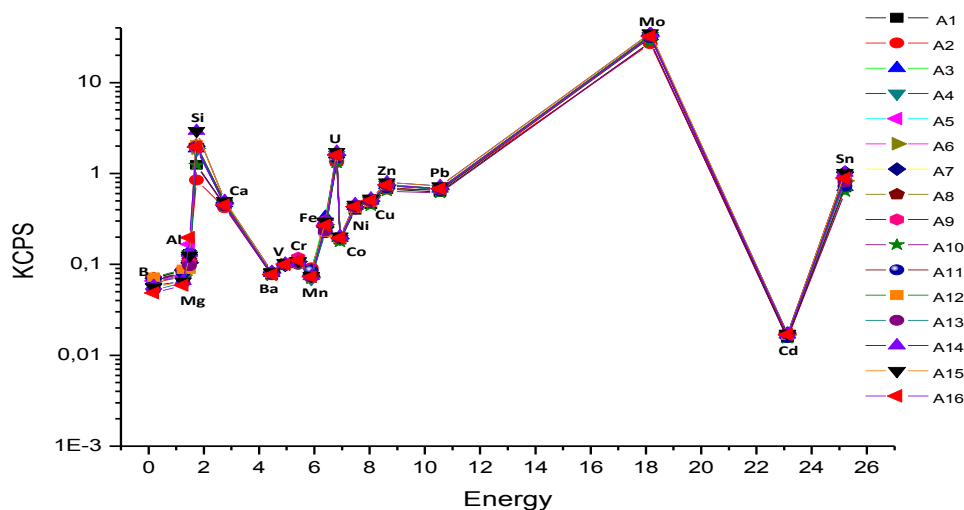
Figure 8: Intensity vs. Energy to obtain an X matrix with U_3Si_2 samples

The PCA analysis revealed two principal components (PC1 = 99.982%; PC2 = 0.016%); however, PC1 is sufficient to describe the calibration model because it has the highest weight (~100%). In Fig 9, the graphic of loading in function of energy calculated for PC1 is shown.
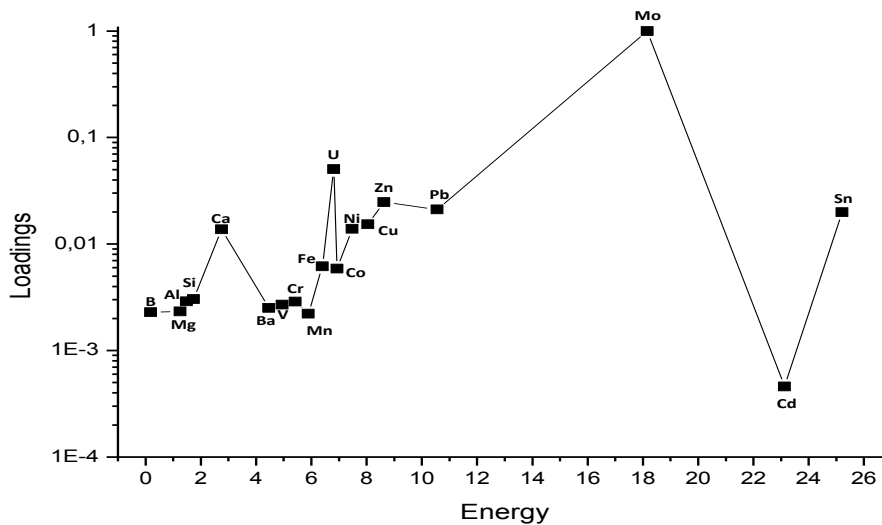
Figure 9: Loading vs. Energy for PC1 in U_3Si_2

Fig. 8 and Fig. 9 have similarities, proving that one component is sufficient to describe the whole range of the U_3Si_2 samples, similar to U_3O_8.

In Table 4, the U_{total} and Si values (average ($\overline{X}$) and variance (σ^2)) were determined by conventional methods ($\overline{X}_V$: volumetric; $\overline{X}_G$: gravimetric). The B, Mg, Al, Si, Ca, V, Cr, Mn, Fe, Co, Ni, Cu, Zn, Mo, Cd, Ba, Sn, and Pb values were determined by ICP-OES ($\overline{X}_{ICP-OES}$) and WDXRF ($\overline{X}_{MC-WDXRF}$) by multivariate calibration. Also, LoQ, Fisher–Snedecor (F) ANOVA, and the student t-test used to compare the difference in outcomes are all presented.

The precision assessment, in relation to ANOVA, showed that the three methods ($\overline{X}_V$: volumetric, $\overline{X}_G$: gravimetric, $\overline{X}_{MC-WDXRF}$) to be statistically equal. The Fisher–Snedecor (F) ANOVA calculated values were lesser than critical F-values for all the elements except Sn (F = 10.03, $_{critical}F$ = 4.96). The student t-test (t) for all the elements was also less than the critical t values.

For the elements where the statistical tests did not apply (B, Mo, Cd, and Ba), because the values were lower than the LoQ, a visual assessment demonstrated their compliance.

The LoQ calculated for the multivariate calibration is sufficient for impurity determination in U_3Si_2 and meets the specifications of U_3Si_2 nuclear fuel.

Table 4: Determined values, LoQ, Fisher–Snedecor (F) ANOVA, and student t-test (t) for U_3Si_2 samples

Element	$\bar{X}_V$ (%)	σ^2	$\bar{X}CM_{-WDXRF}$ (%)	σ^2	LoQ ($\mu g\ g^{-1}$)	F	$_{critical}F$	t	$_{critical}t$	n
U	91.3	0.2	91.8	5.6	1	0.6	4.5	0.8	2.1	16

Element	$\bar{X}_G$ (%)	σ^2	$\bar{X}_{CM-FRX}$ (%)	σ^2	LQ ($\mu g\ g^{-1}$)	F	$F_{crítico}$	t	$t_{crítico}$	n
Si	7.79	0.02	7.82	0.04	1	0.2	4.2	0.5	2.1	16

Elements	$\bar{X}_{ICP-OES}$ ($\mu g\ g^{-1}$)	σ^2	$\bar{X}CM_{-WDXRF}$ ($\mu g\ g^{-1}$)	σ^2	LQ ($\mu g\ g^{-1}$)	F	$F_{crítico}$	t	$t_{crítico}$	n
B	1.5	1.6	<4	NC	4	NC	NC	NC	NC	10
Mg	12.4	188.3	7.1	10.5	1	2.2	4.2	1.6	2.1	16
Al	260	128936	260	25022	23	0.1	4.2	0.1	2.1	16
Ca	11.8	147.2	10.0	42.4	1	0.3	4.2	0.7	2.1	16
V	1.8	5.8	1.8	1.4	2	0.1	4.2	0.2	2.1	16
Cr	25	836	15	46	2	1.9	4.2	1.6	2.1	16
Mn	56	3688	80	2591	8	0.2	4.2	1.0	2.1	16
Fe	283	53059	188	8647	12	2.3	4.2	0.1	2.1	16
Co	14	2	18	2	1	0.2	4.6	0.4	2.4	8
Ni	22	336	30	290	3	1.4	4.2	1.5	2.2	14
Cu	27	264	39	648	4	2.4	4.2	1.7	2.1	16
Zn	14	310	10	40	3	0.6	4.2	0.9	2.1	16
Mo	<3.0	NC	<1	NC	1	NC	NC	NC	NC	16
Cd	<0.1	NC	<2	NC	2	NC	NC	NC	NC	12
Ba	<0.2	NC	<10	NC	10	NC	NC	NC	NC	14
Sn	39	698	78	214	1	10.03	4.96	2.4	2.8	5
Pb	7.9	5.6	9.4	0.4	1	1.3	7.7	1.1	4.3	3

n = number of observations; NC = not calculated

4. CONCLUSIONS

The methodology proposed in this work would allow agencies to meet the requirements for nuclear materials control in relation to U_{total} and impurities in nuclear fuel that is based on U_3Si_2, enriched by 20 wt% ^{235}U, and U_3O_8, in accordance with ISO/IEC 17025.
The method has minimal waste production, reducing analysis time and cost significantly. It also has promise as a method for chemical characterization of materials in nuclear fuel.

ACKNOWLEDGMENTS

REFERENCES

1. "Revista Brasil Nuclear", **v. 19** n. 40, pp.8-11 (2013).
2. "Fonte Nuclear", n.3,"http://www.aben.com.br/ publicacoes/fonte-nuclear/00000000035/combustvel-desenvolvido-no-ipen-poder-ser-utilizado-no-rmb/00000000108" (2012).
3. A.M. Saliba Silva; M. Durazzo; E.F.U. Carvalho; H.G. Riella, "Fabrication of U_3Si_2 powder for fuels in IEA-R1 nuclear research reactor", International Latin-American Conference on Powder Technology, Buzios, RJ. 2007, pp.7-10 (2007).
4. F. B.J. Ferrufino, "Determinação quantitativa da homogeneidade da distribuição de urânio em combustíveis nucleares tipo placa", Dissertação (Mestrado). Instituto de Pesquisas Energéticas e Nucleares, São Paulo (2011).
5. M. Gopalkrishnnan; K. Radhakrishnnan; P. S. Dhami; V. T. Kulkarni; M. V. Joshi; A. B. Patwardhan; J. N Mathur, "Determination of trace impurities in uranium, thorium and plutonium matrices by solvent extraction and inductively coupled plasma atomic emission spectrometry", *Talanta*, **v. 44**, n.2, pp.169–176 (1997).
6. A. L. Souza; M. E. B. Cotrim; M. A. F. Pires, "An overview of spectrometric techniques and sample preparation for the determination of impurities in uranium nuclear fuel grade", Microchemical Journal., doi: 10.1016/j.microc.2012.06.015 (2012).
7. P. Verma; K.L. Ramakumar. "Determination of alkali and alkaline earth elements along with nitrogen in uranium based nuclear fuel materials by ion chromatography (IC)", *Analytica Chimica Acta*, n 601, pp.125–129 (2007).
8. G. V. Ramanaiah, "Determination of ytrium, scandium and other rare earth elements in uranium-rich geological materials by ICP-AES", *Talanta*, **v.46**, n.4, pp.533–540 (1998).
9. R. K. Malhotra; K. Satyanarayana, "Estimation of trace impurities in reactor-grade uranium using ICP-AES", *Talanta*, **v. 50**, n.(3), pp.601–608 (1999).
10. K. Satyanarayana; S. Durani , "Separation and inductively coupled plasma optical emission spectrometric (ICP-OES) determination of trace impurities in nuclear grade uranium oxide", *Journal of Radioanalytical and Nuclear Chemistry*, **v. 285**, n. 3, pp.659–665. (2010).
11. Z. Sulcek; P. Povondra, "Methods of Decomposition". *Analytical Chemistry*, CRC Press, Boca Raton, Florida (1989).
12. M. A. Z. Arruda, "Trends in sample preparation", Nova Science Publishers, New York, USA (2006).
13. J.S. Santos; L.S.G. Teixeira; W.N.L. Santos; V.A. Lemos; J.M. Godoy; S.L.C. Ferreira, "Uranium determination using atomic spectrometric techniques: An overview", *Analytica Chimica Acta*, **v. 674**, n. 2, pp.143–156 (2010).
14. C.H. Knight; R.M. Cassidy; B.M. Recoskie; L.W Green, "Dynamic Ion-Exchange Chromatography for Determination of Number of Fissions in Thorium Uranium-Dioxide Fuels", *Analytical Chemistry*. **v. 56**, n.3, pp.474–478 (1984).

15. S. Bürger; K. J. Mathew; P. Mason; U. Narayanan, "Reference materials characterized for impurities in uranium matrices: An overview and re-evaluation of the NBL CRM 124 series", *Journal of Radioanalytical and Nuclear Chemistry*, **v. 279**, n.2, pp. 659–673 (2009).

16. M. A. Scapin; V. L. R. Salvador; M. E. B. Cotrim; M. A. F. Pires; I. M. Sato, "Uncertainty measurement evaluation of WDXRF and EDXRF techniques for the Si and Utotal determination in U3Si2 nuclear fuel". *Journal of radioanalytical and nuclear chemistry*, **v. 287**, n. 03, pp. 807-811 (2011).

17. "Orientação sobre validação de métodos analíticos": Instituto Nacional de Metrologia, Normalização e Qualidade Industrial – INMETRO, (DOQ-CGRE-008). "http://www.inmetro.gov.br/Sidoq/Arquivos/ CGCRE/DOQ/DOQ-CGCRE-8_03.pdf" (2010).

18. R. Rousseau, "Detection limit and estimate of uncertainty of analytical XRF result", The Rigaku Journal, **v. 18**, n. 2, "http://www.rigaku.com/downloads/journal/Vol18.2.2001/Rousseau.pdf" (2001).

19. M.M.C. Ferreira; A.M. Antunes; M. S. Melgo; P. L. O Volpe, "Quimiometria I: calibração multivariada, um tutorial". *Química Nova*, **v. 22**, n. 5: pp.724-731 (1999).

20. "Quantifying Uncertainty in Analytical Measurement", EURACHEN/CITAC GUIDE, 2ª Edit (2000).

21. T. F. Parreira, "Utilização de métodos quimiométricos em dados de natureza multivariada", Dissertação (Mestrado), Instituto de Química da Universidade de Campinas. Campinas (2003).